Research Square

Preprints are preliminary reports that have not undergone peer review.
They should not be considered conclusive, used to inform clinical practice,
or referenced by the media as validated information.

Identifying Biomarkers for Early Prediction of Coronary Artery Lesions and Intravenous Immunoglobulin Non-response in Kawasaki Disease Based on Urine Multi-omics Analysis

Xiangfan Zeng
Jiangxi Provincial Children's Hospital
Peng Yu
Jiangxi Provincial Children's Hospital
Manying Shi
Jiangxi Provincial Children's Hospital
Junkai Duan
Jiangxi Provincial Children's Hospital
Jiyi Huang
jxsetyyhjy@163.com
Jiangxi Provincial Children's Hospital

Research Article

Keywords: Kawasaki disease, coronary artery lesions, IVIG non-response, multi-omics analysis, biomarkers

Posted Date: July 18th, 2026

DOI: https://doi.org/10.21203/rs.3.rs-10330282/v1

License: This work is licensed under a Creative Commons Attribution 4.0 International License.
Read Full License

Additional Declarations: No competing interests reported.

Abstract

To identify potential biomarkers for predicting coronary artery lesions (CAL) and intravenous immunoglobulin (IVIG) resistance in Kawasaki disease (KD) using integrated metabolomic and proteomic profiling of urine samples.

Methods: Urine samples from 27 pediatric KD patients (13 CAL, 14 NCAL; 5 IVIG non-responders, 5 responders) were analyzed via LC-MS/MS-based non-targeted metabolomics and data-independent acquisition (DIA) proteomics. Differential metabolites (DEMs) and proteins (DEPs) were identified based on fold change >1.5 or <1/1.5 and $p < 0.05$. Functional enrichment and correlation analyses were performed using KEGG and Spearman methods.

Results: In the CAL group, 83 DEMs and 360 DEPs were identified. Integrated analysis revealed three core proteins (APRT, PNP, HPRT1) and three metabolites (guanosine, hypoxanthine, cGMP) linked to purine metabolism and ferroptosis. In IVIG non-responders, guanine was highlighted as a key metabolite, with tryptophan metabolism being the most relevant pathway.

Conclusion: APRT, PNP, HPRT1, guanosine, hypoxanthine, and cGMP may serve as predictive biomarkers for CAL, while guanine shows potential for early detection of IVIG non-response.

Impact

1.Urinary APRT, PNP, HPRT1, guanosine, hypoxanthine, and cGMP are potential early biomarkers for CAL in Kawasaki disease.

2.Guanine alone also predicts IVIG non-response, which is associated with worse outcomes.

3.This is the first urine-based multi-omics (metabolomics + proteomics) study in KD, highlighting purine metabolism and ferroptosis in CAL and tryptophan metabolism in IVIG resistance.

1. Introduction

Systemic vasculitis is the hallmark of Kawasaki disease (KD), an acute febrile sickness. Approximately 25% of patients experience cardiovascular problems, such as coronary artery lesions (CAL), coronary artery aneurysms, and, in severe cases, acute myocardial infarction, if therapy is delayed[2,3]. The established standard for treating the condition involves the use of high-dose intravenous immunoglobulins (IVIG) in conjunction with aspirin. Administering IVIG promptly can provide relief from acute symptoms and has been shown to significantly lower the likelihood of developing CAL[2]. Nevertheless, nearly 15–20% of affected individuals fail to exhibit an adequate response after receiving the first course of IVIG; instead, they sustain either prolonged or relapsing pyrexia lasting a minimum of 36 h following completion of the initial infusion. Prior research has indicated that resistance to the first IVIG dose correlates with heightened risks for coronary artery lesions (CAL) and severe adverse events[4],

such as KD shock syndrome (KDSS) and KD-related macrophage activation syndrome. Therefore, the early identification of biomarkers that can predict the occurrence of coronary artery lesions in KD and IVIG non-responders is crucial for clinical diagnosis and intervention.

Numerous studies have investigated KD-related biomarkers, some of which have demonstrated predictive value for IVIG non-response or an increased risk of CAL. The specificity and sensitivity of these biomarkers are suboptimal[1].In addition, most biomarker studies are based on blood samples. However, due to physiological homeostatic mechanisms that regulate and eliminate harmful substances, the window period for identifying blood biomarkers is limited. Considering the invasiveness and limitations associated with blood collection, urine represents an attractive alternative source for biomarker identification.

Urine is produced via ultrafiltration by the kidneys. The concentration of certain biomarkers (such as hormones and small-molecule metabolites) is higher in the urine than in the blood. Unlike the high variability in protein concentrations in the blood ($0–10^{12}$), the variability in urine protein concentration is limited ($10^{5}–10^{6}$), because of which proteins with biomarker significance are not masked by high-abundance proteins[5]. Additionally, unlike blood, urine is not subject to homeostatic control and its composition can reflect minor systemic changes[6]. As a non-invasively collected bodily fluid sample, urine can be conveniently used for dynamic clinical analysis and monitoring of disease progression. Currently, disease biomarkers in urine samples are being investigated extensively. For example, the Bence Jones protein can assist in the diagnosis of multiple myeloma[7]; urinary proteins such as CDC5L, ITIH2, AFM, CFL1, APOA1, A2M, FGB, and CD5L can act as potential biomarkers for bladder cance[8]; and TIMP1, MMP2, and vWF can aid in diagnosing coronary artery disease complicated by aortic valve stenosis[9].

We aimed to conduct an integrated analysis of untargeted metabolomics data generated by liquid chromatography–tandem mass spectrometry (LC–MS/MS) and quantitative proteomics data obtained using data-independent acquisition (DIA) mass spectrometry in urine samples from children with KD. By comparing patients with and without CAL, as well as IVIG responders and non-responders, we aimed to identify potential biomarkers with predictive value for early-stage coronary artery injury and IVIG resistance. Our observations may provide an early warning for IVIG resistance in children with KD.

2. Materials and Methods

This work enrolled 27 children diagnosed with KD, among whom 13 developed CAL and 14 did not (NCAL). Among the 27 patients, 5 patients with KD were classified as IVIG non-responders. The inclusion criteria were: age 0–16 years; KD diagnosis following the criteria of the 2017 American Heart Association of Cardiology modified guidelines; treatment with IVIG (2 g/kg) and high-dose aspirin (30–50 mg/kg/day) for 72 h to maintain a normal body temperature, followed by low-dose aspirin (3–5 mg/kg/day); patients who underwent echocardiographic examinations during the acute, subacute, and recovery phases, with complete records available.

Definition of CAL: A Z-score of the left or right coronary artery ≥ 2.5, a coronary artery diameter ≥ 3 mm (or ≥ 4 mm in children aged > 5 years), or a dilated coronary segment with a diameter > 1.5-fold that of the adjacent segment.

Definition of IVIG non-response: Persistent fever (> 38°C) at least 36 h after the initial IVIG administration or recrudescent fever within 2 weeks of treatment, accompanied by at least one major clinical manifestation of KD, after exclusion of other potential causes of fever[10].

The following exclusion criteria were applied: inability to definitively diagnose KD, incomplete clinical data, failure to undergo standard echocardiographic evaluation for CAL, prior history of KD, concomitant cardiovascular disease or other rheumatic/immune-mediated diseases, and children with congenital renal or urinary tract structural abnormalities, urinary tract infections, acute or chronic nephritis or nephrotic syndrome, nephritis caused by autoimmune diseases, urinary system tumors, adrenal diseases, hypothalamic or pituitary diseases, other suspected genetic metabolic disorders, and immune deficiency.

2.2 Urine Sample Preparation

Following perineal cleansing, midstream urine specimens were obtained from each patient in the morning. Within 2 h post-collection, the samples were kept at 4°C and then centrifuged at 5,000 ×g for 30 min. The resultant supernatant was decanted into a cryovial, snap-frozen in liquid nitrogen for 2 min, and finally preserved at − 80°C until further analysis.

2.3 Metabolite Extraction and LC–MS Analysis

To extract metabolites, 300 µL of ice-cold methanol was added to 100 µL of urine. The mixture was held at − 20°C for 30 min, followed by centrifugation at 16,000 ×g for 20 min (4°C). The resulting supernatant was subjected to LC–MS analysis. LC–MS separation was performed on a Shimadzu LC-30 AD system (Kyoto, Japan) equipped with an ACQUITY UPLC® HSS T3 column (2.1 × 100 mm, 1.8 µm; Waters, Milford, MA, USA) thermostated at 45°C. Mobile phase A was water with 0.1% formic acid, while mobile phase B was acetonitrile with 0.1% formic acid. The gradient program was set as follows: 0–1 min, 5% B; 1–16 min, 5–95% B; 16–17 min, 95–5% B. Mass spectrometry was performed using an Exactive™ Plus Hybrid Quadrupole-Orbitrap™ instrument (Thermo Scientific, Waltham, MA) equipped with an electrospray ionization source operating in both positive and negative ion modes. The resolution for MS^1 scans was configured at 70,000, and the spectral acquisition covered a mass-to-charge ratio (m/z) range of 75–1000.

2.4 Metabolomic Data Processing

Raw LC–MS data were processed by MS-DIAL (version 4.8) for peak detection, alignment, retention-time correction, and compound identification based on public metabolomic databases (HMDB, MoNA). Finally, the peak intensity matrix was normalized by unit variance scaling and log transformation. Multivariate statistical modeling including PCA and PLS-DA was performed in MetaboAnalyst 5.0.

Differential metabolites were chosen using the criteria of variable importance in projection (VIP) > 1.5 and $p < 0.05$ (Student's t-test or Mann–Whitney U test).

2.5 Statistical and Functional Analysis

Univariate comparisons were carried out with either parametric or non-parametric methods, chosen according to the distribution of the data. Spearman's rank correlation was applied to evaluate relationships between metabolite concentrations and clinical traits. Significantly perturbed metabolic pathways were identified via Kyoto Encyclopedia of Genes and Genomes (KEGG) pathway enrichment analysis. For all statistical tests, significance was defined as $p < 0.05$.

3. Results

3.1 Data Analysis of the CAL-NCAL Groups

3.1.1 Clinical Data Analysis

As presented in Table 1, CAL and NCAL groups showed comparable baseline characteristics, with no statistically significant differences in age, sex, body weight, or clinical parameters including hepatic, renal, and cardiac function, as well as routine blood and urinalysis results (all $P > 0.05$).

Table 1
Comparison of clinical data between CAL and NCAL groups

Age (months)	**CAL(*N* = 13)**	**NCAL(*N* = 14)**	***P-value***
	34.5 ± 25.2	***36.1 ± 16.1***	**0.970**
Sex (m/f)	9/4	8/6	0.802
Weight (kg)	*13.0(10.5,16.5)*	*13.6 ± 2.6*	0.954
Thermal range (days)	*5.3 ± 2.1*	*5.5(4.3,7.0)*	0.396
WBC (10^9/L)	*16.3(11.8, 22.3)*	*15.7 ± 4.7*	0.686
PLT (10^9/L)	*341.2 ± 98.8*	*299.5(283.3,374.3)*	0.795
HB (g/L)	*109.1 ± 14.3*	*115.3 ± 8.0*	0.271
NE (10^9/L)	*11.8(8.2,18.0)*	*11.6 ± 5.1*	0.954
LYM (10^9/L)	*2.9 ± 1.7*	*2.8 ± 1.1*	0.823
RBC (10^{12}/L)	*4.1 ± 0.4*	*4.2 ± 0.2*	0.329
ALT (U/L)	*54.0(15.7,140.8)*	*41.5 ± 30.5*	0.225
AST (U/L)	*42.9(29.9,50.0)*	*33.4(22.3,43.7)*	0.184
LDH (U/L)	*264.5(239.4,276.9)*	*242.4 ± 50.6*	0.260
CK (U/L)	*28(18.1,81.8)*	*45.5 ± 22.6*	0.583
CK-MB (U/L)	*10.9 ± 4.0*	*9.15(6.6,11.6)*	0.908
BUN (mmol)	*2.6(2.3,4.0)*	*3.3 ± 1.2*	0.773
CR (μmol)	*26.7(23.3,29.3)*	*27.1 ± 5.5*	0.644
UA (μmol)	*176.6(162.4,267.2)*	*220.5 ± 87.1*	0.908
CRP (mg/L)	*99.2 ± 64.4*	*89.0 ± 48.5*	0.545
SAA (mg/L)	*256.2(230.8,458.6)*	*239.6(192.3,506.4)*	0.603
Urine specific gravity	*1.015(1.010,1,015)*	*1.010(1.010,1.010)*	0.981
Urine pH	*6.4 ± 0.3*	*6.5(6.0,7.0)*	0.650
Erythrocytes in urine			
Negative	13(100%)	13(92.9%)	0.756
Positive 2+	0(0%)	1(7.1%)	
Urinary white blood Cells (negative)	13(100%)	14(100%)	1.000

3.1.2 Analysis of the Metabolomics and Proteomics Data of the CAL-NCAL Group

The metabolomic PLS-DA score plot for the CAL-NCAL group is shown in Fig. 2a. The two groups were clearly separated, and the differences between them were significant. The proteomic PCA score plot for the CAL-NCAL group is shown in Fig. 2b. There was a partial overlap between the data of the two groups, and the differences between the groups were not significant, indicating that the two sets of data may share common protein phenotypes.

In total, 83 differentially expressed genes (DEMs) were identified in the CAL-NCAL group, including 66 up-regulated DEMs and 17 down-regulated DEMs. As shown in Fig. 2d, the metabolites, lysophosphatidylcholine (LPC (16:0)), nicotinamide, palmitic amide, isoflavone B, and triglyceride (18:1/18:1/18:1) were significantly upregulated in the CAL group, while phosphatidylcholine (PC (18:0/18:2), PC (16:0/18:1), and PC (16:0/16:0) were significantly downregulated in the CAL group.

KEGG enrichment analysis of these DEMs revealed that the top 10 pathways with the most significant differences ($P < 0.05$) were purine metabolism, nucleotide metabolism, folate biosynthesis, olfactory transmission, light transmission, circadian rhythm regulation, major depressive disorder, cGMP-PKG signaling pathway, parathyroid hormone synthesis, secretion, and action, and gap junctions (Fig. 2c).

In total, 360 DEPs were identified in the CAL-NCAL group, including 207 up-regulated DEPs and 153 down-regulated DEPs. Moreover, the further KEGG analysis of DEPs showed that they were enriched in tyrosine metabolism, starch and sucrose metabolism, purine metabolism, pantothenic acid and CoA biosynthesis, nucleotide metabolism, nicotinic acid and nicotinamide metabolism, glycolysis/ glycogen synthesis, fructose and mannose metabolism, cysteine and methionine metabolism and β-alanine metabolism pathways. (Fig. 2e).

3.1.3 An integrative multi-omics study of the proteome and metabolome in the CAL-NCAL Group

We performed integrated proteomic-metabolomic profiling between the CAL and NCAL groups at the expression level (Fig. 3a) and pathway (KEGG) level (Fig. 3b) to screen for core molecules. These included the proteins adenine phosphoribosyltransferase (APRT), purine nucleoside phosphorylase (PNP), and hypoxanthine phosphoribosyltransferase 1 (HPRT1), as well as the metabolites guanosine, hypoxanthine, and 3',5'-cyclic guanosine monophosphate (3',5'-cGMP). KEGG analysis of DEMs and DEPs jointly enriched 22 pathways, among which purine metabolism, ferroptosis, and cysteine and methionine metabolism were significantly altered ($P < 0.05$).

Receiver operating characteristic (ROC) analysis was performed on the three core metabolites and proteins to assess their predictive value (Fig. 3). In the CAL group, the expression levels of the proteins

APRT, PNP, and HPRT, as well as the core metabolites, guanosine, hypoxanthine, and 3',5'-cGMP, were significantly higher than those in the NCAL group (Fig. 4).

3.2. Data Analysis of IVIG-resistance and IVIG-sensitive Groups

3.2.1 Clinical Data Analysis

Age, sex, or weight did not differ significantly between the IVIG-resistant and IVIG-sensitive groups; there were no significant differences in liver, kidney, and heart function, blood counts, or results of urine test (Table 2).

Table 2
Analysis of clinical data in IVIG-resistant and IVIG-sensitive groups

Age (months)	**IVIG-resistance(*N* = 5)**	**IVIG-sensitive(*N* = 5)**	***P-value***
	32.8 ± 21.1	***31 ± 15.9***	**0.883**
Sex (m/f)	4/1	4/1	1.000
Weight (kg)	*13.1 ± 3.1*	*12.8 ± 2.7*	0.873
Thermal range (days)	*4.6 ± 1.1*	*4.0(4.5, 7.0)*	0.133
WBC (10^9/L)	*16.0 ± 5.1*	*13.9 ± 3.8*	0.497
PLT (10^9/L)	*314.8 ± 29.2*	*355.0 ± 80.1*	0.323
HB (g/L)	*119.6 ± 9.1*	*108.8 ± 10.6*	0.121
NE (10^9/L)	*12.6 ± 5.4*	*8.5(7.1, 13.0)*	0.375
LYM (10^9/L)	*2.4 ± 0.9*	*2.8 ± 1.2*	0.556
RBC (10^{12}/L)	*4.4 ± 0.3*	*4.0 ± 0.2*	0.059
ALT (U/L)	*69.0(37.0,574.9)*	*40.3 ± 21.2*	0.251
AST (U/L)	*36.0(19.0,264.9)*	*30.6 ± 11.0*	0.675
LDH (U/L)	*273.0(268.0,289.5)*	*229.0(125.2, 268.0)*	0.075
CK (U/L)	*36.9 ± 26.1*	*44.0 ± 19.9*	0.640
CK-MB (U/L)	*9.2 ± 2.8*	*7.8 ± 2.9*	0.466
BUN (mmol)	*2.3 ± 0.9*	*3.0 ± 1.7*	0.600
CR (μmol)	*26.5 ± 5.9*	*25.8 ± 5.7*	0.873
UA (μmol)	*204.3 ± 38.3*	*153.7(135.5, 243.9)*	0.175
CRP (mg/L)	*91.4 ± 37.6*	*64.4 ± 38.4*	0.294
SAA (mg/L)	*234.2(220.3,30.3)*	*256.0(206.0, 349.4)*	0.754
Urine specific gravity	*1.013 ± 0.004*	*1.016 ± 0.005*	0.421
Urine pH	*6.5 ± 0.4*	*6.7 ± 0.4*	0.421
Red blood cells in urine (negative)	5(100%)	5(100%)	1.000
Urinary leukocytes (negative)	5(100%)	5(100%)	1.000

3.2.2. Analysis of the Metabolomics and Proteomics Data of the IVIG-resistance and IVIG-sensitive Groups

The PLS-DA score plots of the metabolomic data for the IVIG-resistant and IVIG-sensitive groups are shown in Fig. 5a. The two groups were clearly separated, and the differences between them were statistically significant. A PCA score plot of the proteomic data for the two groups is shown in Fig. 5b. There was an overlap between the two datasets, which may be related to the small sample sizes.

In total, 64 DEMs were identified in the IVIG-resistant versus IVIG-sensitive groups, including 30 up-regulated and 34 down-regulated DEMs. KEGG analysis showed that DEMs were primarily enriched in vitamin B6 metabolism, tyrosine metabolism, tryptophan metabolism, pyrimidine metabolism, phenylalanine metabolism, pantothenic acid and CoA biosynthesis, glycerolipid metabolism, glycerophospholipid metabolism, and β-alanine metabolism (Fig. 5c).

In total, 123 DEPs were identified in the IVIG resistance-IVIG sensitive group, including 88 up-regulated and 35 down-regulated DEPs. KEGG analysis of the DEPs revealed enrichment in pathways such as the interconversion of pentoses and glucuronic acid; fatty acid degradation; valine, leucine, and isoleucine degradation; and fatty acid metabolism (Fig. 5d).

In our study, some patients with KD did not respond to IVIG administration. To further identify biomarkers that could predict the occurrence of IVIG non-response, we used the MetaboAnalyst website to perform a correlation analysis of DEMs and DEPs between the IVIG non-response and IVIG-sensitive groups (Fig. 6a). We found that metabolites centered around guanine, proteins, XDH and RHOB, were closely associated with guanine. Additionally, we conducted a joint analysis of the KEGG pathways enriched in DEMs and DEPs (Fig. 6b). The two groups were jointly enriched in nine pathways: tryptophan metabolism, β-alanine metabolism, pantothenic acid and CoA biosynthesis, glycerophospholipid metabolism, chemical carcinogenesis—reactive oxygen species, protein digestion and absorption, metabolic pathways, lysine degradation, and cofactor biosynthesis.

ROC curve analysis was performed on the selected key metabolite guanosine, yielding an area under the curve of 0.84. The comparison revealed that the guanosine expression levels were significantly higher in the IVIG-resistant group than in the IVIG-sensitive group (Fig. 7).

4. Discussion

In total, 83 DEMs and 360 DEPs were identified in the CAL-NCAL group. Based on expression levels, a joint analysis identified three core proteins (APRT, PNP, and HPRT1) and three core metabolites (guanosine, hypoxanthine, and 3',5'-cyclic GMP). Joint analysis at the KEGG level revealed 22 shared pathways, with the most significantly altered pathways being purine metabolism, ferroptosis, and cysteine and methionine metabolism ($P < 0.05$).

In the IVIG-resistance-IVIG-sensitive group, 64 metabolites and 123 proteins were screened, and based on the expression level in joint analysis, the core metabolite, guanine, was screened. Similarly, based on KEGG pathway joint analysis, nine common pathways were identified. We focused on the tryptophan metabolism pathway.

In the CAL-NACL group, we identified three core proteins (APRT, PNP, and HPRT1) and three core metabolites (guanosine, hypoxanthine, and 3',5'-cyclic guanosine monophosphate), all of which are closely related to purine metabolism. Previous studies have demonstrated that ATP can activate immune cells by stimulating them and induce the expression of pro-inflammatory cytokines, such as interleukin-1β (IL-1β), interleukin-6 (IL-6) and tumor necrosis factor-α (TNF-α)[11].ATP is sequentially hydrolyzed into ADP and AMP, which are then phosphorylated to adenosine by APRT. Adenosine exerts significant anti-inflammatory effects[12]. HPRT1, a key enzyme in the purine salvage pathway, plays an important role in maintaining intracellular purine homeostasis. These findings suggest that purine metabolic pathway play an important role in immune regulation in the CAL-NACL group.

Furthermore, triglyceride, LPC, and 3-hydroxy-2-oxoglutarate metabolites were significantly upregulated in the CAL group. The first two are involved in glycerophospholipid metabolism, and blood lipids are key factors involved in the onset of cardiovascular events. A retrospective study by Zhang et al. [13] showed that triglyceride and low-density lipoprotein levels were elevated during the acute phase of KD and that triglyceride levels were associated with CAL severity. This potential mechanism may be related to increased oxidative stress levels in children with KD. Enhanced oxidative stress can exacerbate lipid peroxidation, promote vascular endothelial cell damage, and reduce protective high-density lipoprotein levels on the surface of vascular endothelial cells, leading to triglyceride deposition on the vascular wall[14]. Lysophospholipids are key signaling molecules involved in regulating inflammatory responses[15]. Serum lysophosphatidylethanolamine (LPE) levels decrease due to inflammatory states such as insulin resistance[16], non-alcoholic steatohepatitis[17], and cancer-related inflammation[18]. Chen et al.[19] showed that LPE and LPC expression decreased after IVIG treatment, possibly due to the suppression of persistent inflammatory responses. This contradicts our findings, which may be because the children in this study had not yet undergone IVIG treatment at the time of sampling.

Our study revealed significant changes in ferroptosis pathways in the CAL group. Ferroptosis is an iron-dependent and lipid peroxidation-driven form of programmed cell death. Our findings showed that triglycerides and LPC were significantly upregulated in the CAL group; however, the mechanism of ferroptosis in KD remains unclear.

Compared with the IVIG-resistant and IVIG-sensitive groups, we found that the tryptophan metabolic pathway was coenriched in DEMs and DEPs. Tryptophan is an indispensable amino acid in the human body, and the L-kynurenine (Kyn) pathway is one of the main ways to break down tryptophan, which can lead to Kyn and its downstream products and participate in inflammatory and immune responses[20]. Xue et al.[21] discovered that the patients with KD had significantly decreased levels of tryptophan and IAA, while the Kyn and kynurenic acid levels were significantly higher than that in healthy controls. Similar changes have been observed in the mouse model of KD coronary arteritis. Kyn promotes the inflammatory vascular disease process of aortic disease[22]. IAA could decrease the inflammation and reactive oxygen species levels by decreasing the expression of the pro-inflammatory cytokines[23]. In the

CAL-NCAL group, we found that the 3-hydroxy-kynurenic acid expression was upregulated[24]. This may cause damage to the coronary artery.

This investigation is constrained by its single-center design and limited cohort size. Future studies should aim to incorporate multi-center collaborations and expand the sample population to enhance statistical power and generalizability. Furthermore, the putative biomarkers identified herein warrant further validation through both in vivo and in vitro experimental approaches to elucidate their functional roles and clinical applicability.

5. Conclusions

APRT, PNP, HPRT1, guanosine, hypoxanthine, and cGMP may serve as predictive biomarkers for CAL, while guanine shows potential for early detection of IVIG non-response.

Abbreviations

The following abbreviations are used in this manuscript:

CAL, coronary artery dilation; KD, Kawasaki disease, IVIG, intravenous immunoglobulin; DEMs, differentially expressed metabolites; DEPs, differentially expressed proteins; LPE, lysophosphatidylethanolamine; LPC, lysophosphatidylcholine

Declarations

Institutional Review Board Statement: This study was conducted in accordance with the Declaration of Helsinki, and approved by the Ethics Committee of Jiangxi Children's Hospital (Ethics Review Approval Number: JXSETYY-YXKY-20240080).Written informed consent was waived, as we only analyzed anonymous residual waste urine specimens without any clinical intervention or adjustment of patients' treatment plans. This research is a non-interventional retrospective study and does not require clinical trial registration.

Informed Consent Statement: Informed consent was obtained from all subjects involved in the study.

Data Availability Statement: The original contributions presented in this study are included in the article/supplementary material. Further inquiries can be directed to the corresponding authors.

Conflicts of Interest: The authors declare no conflict of interest.

Funding: This research was funded by the Science and Technology Plan of Health Commission of Jiangxi Province (No. 202610765), the Science and Technology Project of Jiangxi Provincial Administration of Tradition-al Chinese Medicine (grant numbers 2023Z016),the Nanchang Key Laboratory of Biological Sample Resource Management and Application, and the JXHC Key Laboratory of Children's Cardiovascular Diseases.

Author Contributions: Concept and design, Huang Ji Yi; Sample collection and Data organization: Zeng Xiang Fan; Formal analysis, Huang Ji Yi and Zeng Xiang Fan; Methodology: Huang Ji Yi; Supervision: Duan Jun Kai; Drafting of the manuscript: Huang Ji Yi and Zeng Xiang Fan; Reviewing and editing: Duan Jun Kai. All authors have read and approved the final manuscript.

Acknowledgments: We thank the patients who participated in this study. We also thank Shanghai Baipu Biotechnology Co., Ltd. (Shanghai, China) for technical support in joint omics. We further thank the editors and peer reviewers for their contributions to this article.

References

1. Sosa T, Brower L, Divanovic A. Diagnosis and Management of Kawasaki Disease. JAMA Pediatr. 2019;173(3):278–9.
2. McCrindle BW, Rowley AH, Newburger JW, Burns JC, Bolger AF, Gewitz M, et al. Diagnosis, Treatment, and Long-Term Management of Kawasaki Disease: A Scientific Statement for Health Professionals From the American Heart Association. Circulation. 2017;135(17):e927–99.
3. Elakabawi K, Lin J, Jiao F, Guo N, Yuan Z. Kawasaki Disease: Global Burden and Genetic Background. Cardiol Res. 2020;11(1):9–14.
4. Zhao L, Wu J, Liu X, Zhou K, Hua Y, Shao S, et al. Risk factors for predicting medium-giant coronary artery aneurysms in Kawasaki disease. Immunol Res. 2025;73(1):52.
5. Hortin GL, Sviridov D. The dynamic range problem in the analysis of the plasma proteome. J Proteom. 2010;73(3):629–36.
6. Gao Y. Urine-an untapped goldmine for biomarker discovery? Sci China Life Sci. 2013;56(12):1145–6.
7. Sewpersad S, Pillay TS. Historical perspectives in clinical pathology: Bence Jones protein-early urine chemistry and the impact on modern day diagnostics. J Clin Pathol. 2021;74(4):212–5.
8. Suh J, Han D, Ku JH, Kim HH, Kwak C, Jeong CW. Next-generation Proteomics-Based Discovery, Verification, and Validation of Urine Biomarkers for Bladder Cancer Diagnosis. Cancer Res Treat. 2022;54(3):882–93.
9. Perpétuo L, Barros AS, Dalsuco J, Nogueira-Ferreira R, Resende-Gonçalves P, Falcão-Pires I et al. Coronary Artery Disease and Aortic Valve Stenosis: A Urine Proteomics Study. Int J Mol Sci. 2022;23(21).
10. Gorelik M, Chung SA, Ardalan K, Binstadt BA, Friedman K, Hayward K et al. 2021 American College of Rheumatology/Vasculitis Foundation Guideline for the Management of Kawasaki Disease. Arthritis & rheumatology (Hoboken, NJ). 2022;74(4):586–96.
11. Linden J, Koch-Nolte F, Dahl G. Purine Release, Metabolism, and Signaling in the Inflammatory Response. Annu Rev Immunol. 2019;37:325–47.
12. Huang Z, Xie N, Illes P, Di Virgilio F, Ulrich H, Semyanov A, et al. From purines to purinergic signalling: molecular functions and human diseases. Signal Transduct Target therapy. 2021;6(1):162.

13. Zhang H, Cai J, Zhang R, Shuai S, Tang M, Ju R, et al. The role of serum lipid in predicting coronary artery lesions and intravenous immunoglobulin resistance in Kawasaki disease: a cohort study. J Int Med Res. 2024;52(5):3000605241252115.
14. Shao S, Zhou K, Liu X, Liu L, Wu M, Deng Y, et al. Predictive Value of Serum Lipid for Intravenous Immunoglobulin Resistance and Coronary Artery Lesion in Kawasaki Disease. J Clin Endocrinol Metab. 2021;106(10):e4210–20.
15. Sevastou I, Kaffe E, Mouratis MA, Aidinis V. Lysoglycerophospholipids in chronic inflammatory disorders: the PLA(2)/LPC and ATX/LPA axes. Biochim Biophys Acta. 2013;1831(1):42–60.
16. Zhang X, Liu H, Li C, Wei Y, Kan X, Liu X et al. Abdominal obesity in youth: the associations of plasma Lysophophatidylcholine concentrations with insulin resistance. Pediatr Res. 2024.
17. Wang J, Li J, Fu Y, Zhu Y, Lin L, Li Y. Research progress, challenges and perspectives of phospholipids metabolism in the LXR-LPCAT3 signaling pathway and its relation to NAFLD (Review). Int J Mol Med. 2024;53(4).
18. Shao G, Qian Y, Lu L, Liu Y, Wu T, Ji G, et al. Research progress in the role and mechanism of LPCAT3 in metabolic related diseases and cancer. J Cancer. 2022;13(8):2430–9.
19. Chen Z, Sai S, Nagumo K, Wu Y, Chiba H, Hui SP. Distinctive serum lipidomic profile of IVIG-resistant Kawasaki disease children before and after treatment. PLoS ONE. 2023;18(3):e0283710.
20. Wang Q, Liu D, Song P, Zou MH. Tryptophan-kynurenine pathway is dysregulated in inflammation, and immune activation. Front bioscience (Landmark edition). 2015;20(7):1116–43.
21. Fan X, Li K, Guo X, Liao S, Zhang Q, Xu Y, et al. Metabolic profiling reveals altered tryptophan metabolism in patients with kawasaki disease. Front Mol Biosci. 2023;10:1180537.
22. Ramprasath T, Han YM, Zhang D, Yu CJ, Zou MH. Tryptophan Catabolism and Inflammation: A Novel Therapeutic Target For Aortic Diseases. Front Immunol. 2021;12:731701.
23. Ji Y, Yin W, Liang Y, Sun L, Yin Y, Zhang W. Anti-Inflammatory and Anti-Oxidative Activity of Indole-3-Acetic Acid Involves Induction of HO-1 and Neutralization of Free Radicals in RAW264.7 Cells. Int J Mol Sci. 2020;21(5).
24. Yang Y, Liu X, Liu X, Xie C, Shi J. The role of the kynurenine pathway in cardiovascular disease. Front Cardiovasc Med. 2024;11:1406856.

Figures

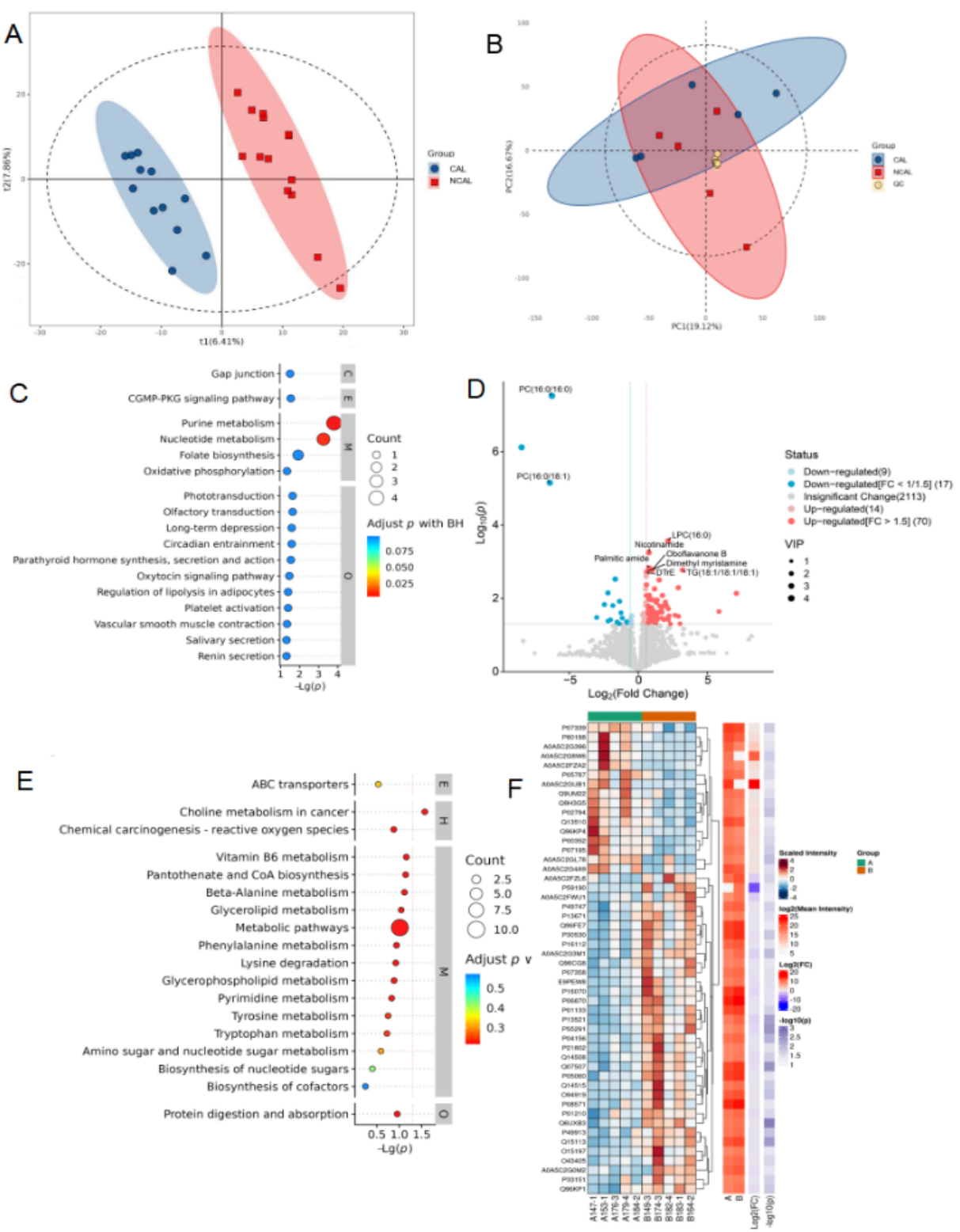


Figure 1

(A) (B): t1 represents principal component 1, t2 represents principal component 2, points of the same color represent various biological replicates within the group, and the distribution of points reflects the degree of difference between and within groups. (C) (E): KEGG pathways enriched with differentially expressed metabolites and proteins, respectively. (D): Volcano plot of the CAL group and NCAL group, with red indicating an increase and blue indicating a decrease, and the size of the dots indicating the VIP

value.(F):Cluster analysis of DEPs :the DEPs were mainly transport proteins (LCN2, FLT), enzyme proteins (MMP7, CTSD, DDAH1, LDHB, CTHRC1), cytoskeletal proteins (KRT8, WDR1), cell signaling proteins (EPDR1, AXL, EGF, FHFR2), and cell adhesion proteins (CDH15, CD44, CDH5).

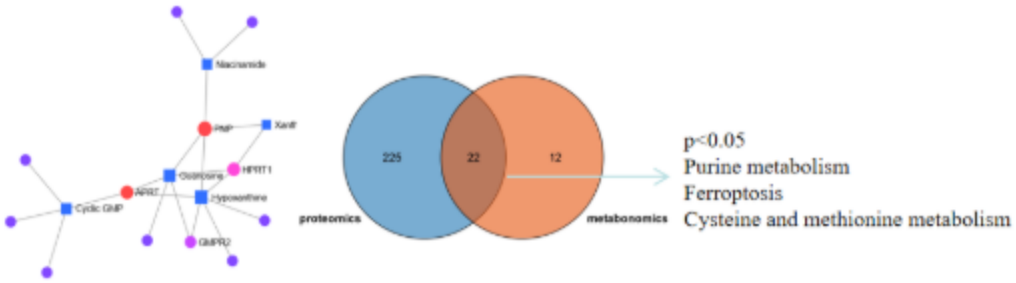


Figure 2

A graph shows the DEMs and DEPs correlation interactions network map of the CAL-NCAL group, and B graph shows the KEGG pathway that DEMs and DEPs are co-enriched to in the CAL-NCAL group.

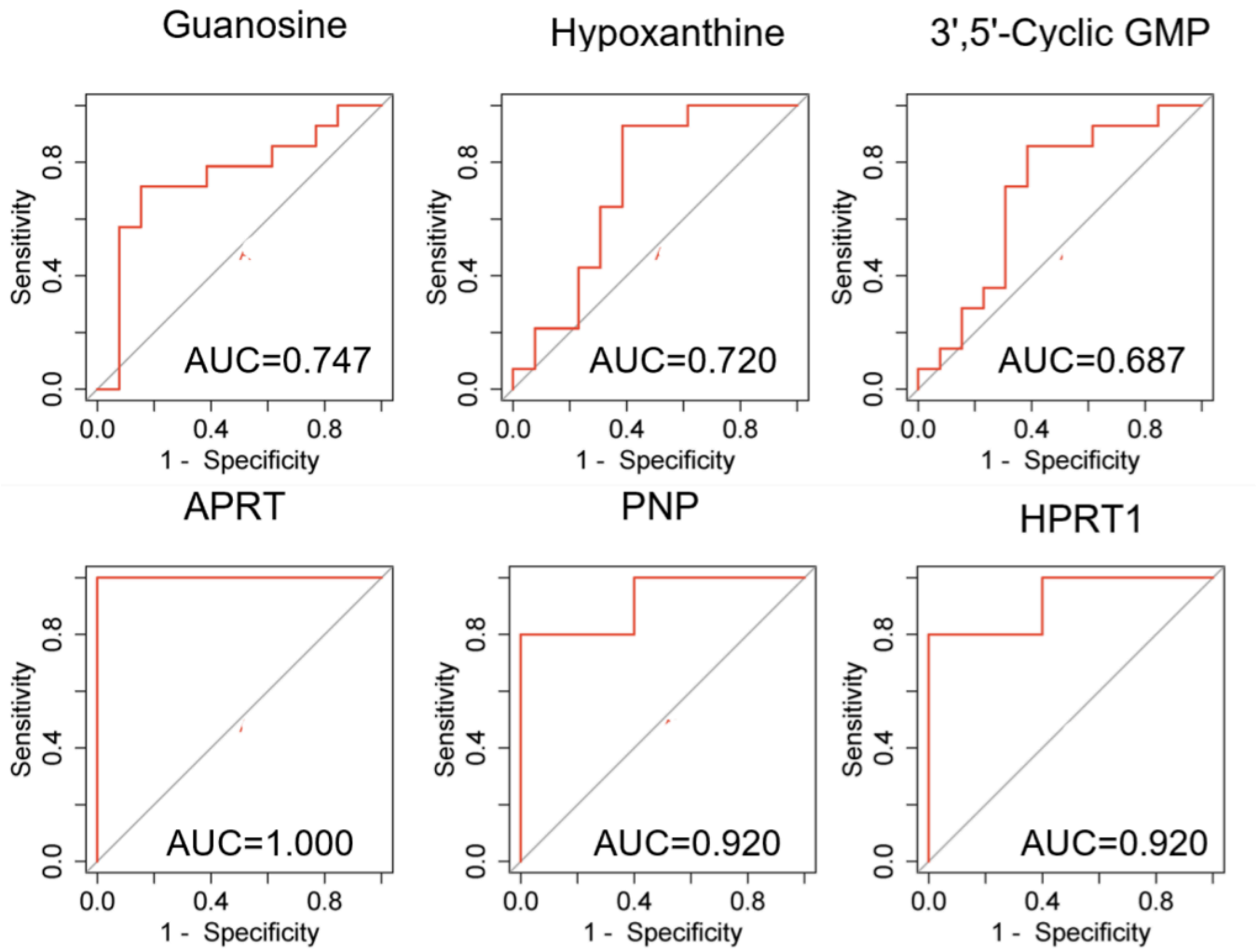


Figure 3

Roc curves of Guanosine, Hypoxanthine, 3‘,5’-Cyclic GMP, APRT, PNP and HPRT1.

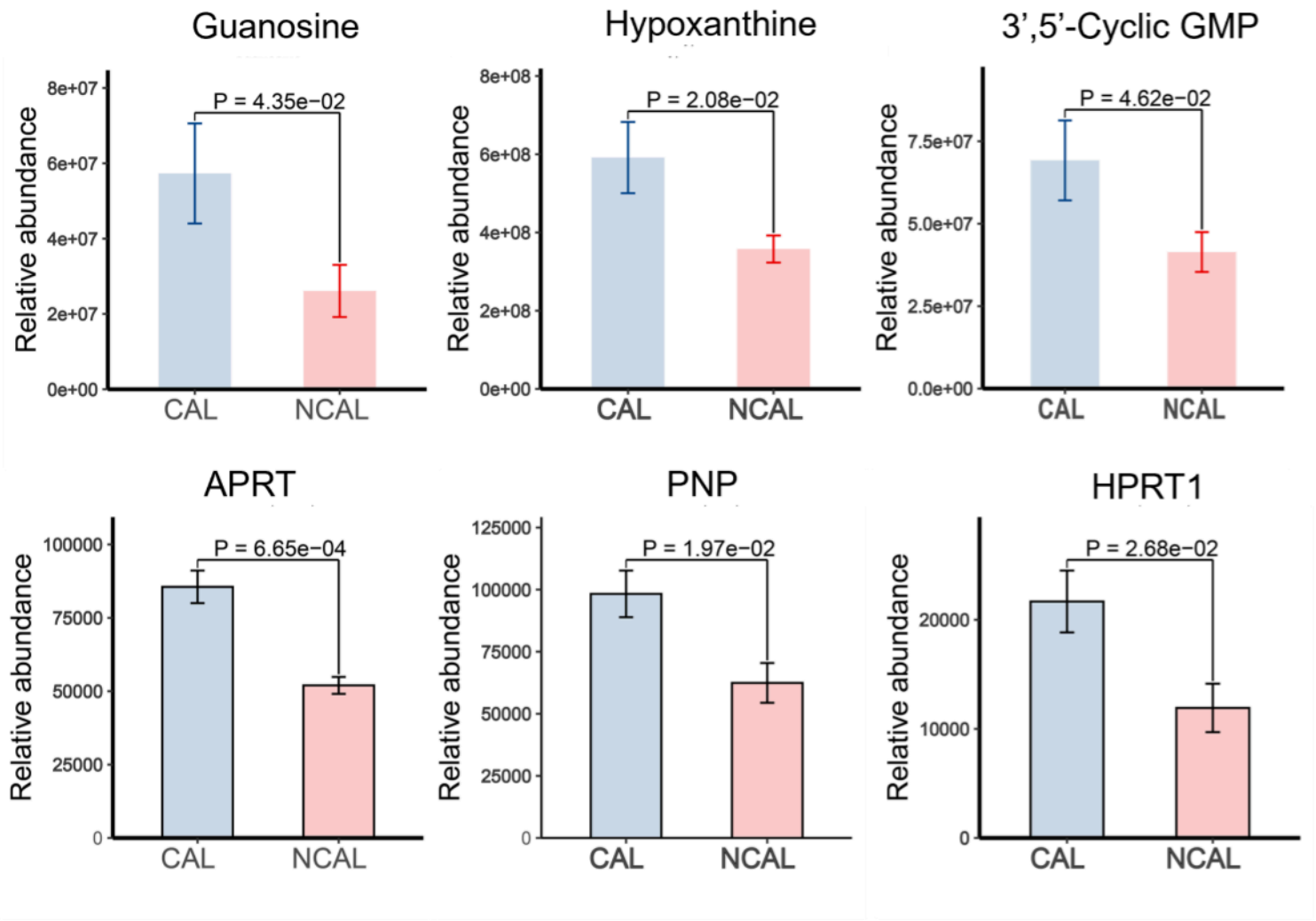


Figure 4

Histogram analysis of the expression of Guanosine, Hypoxanthine, 3‘,5’-Cyclic GMP, APRT, PNP and HPRT1 in the CAL and NCAL groups, where group I and A represents the CAL group and group II and B represents the NCAL group.

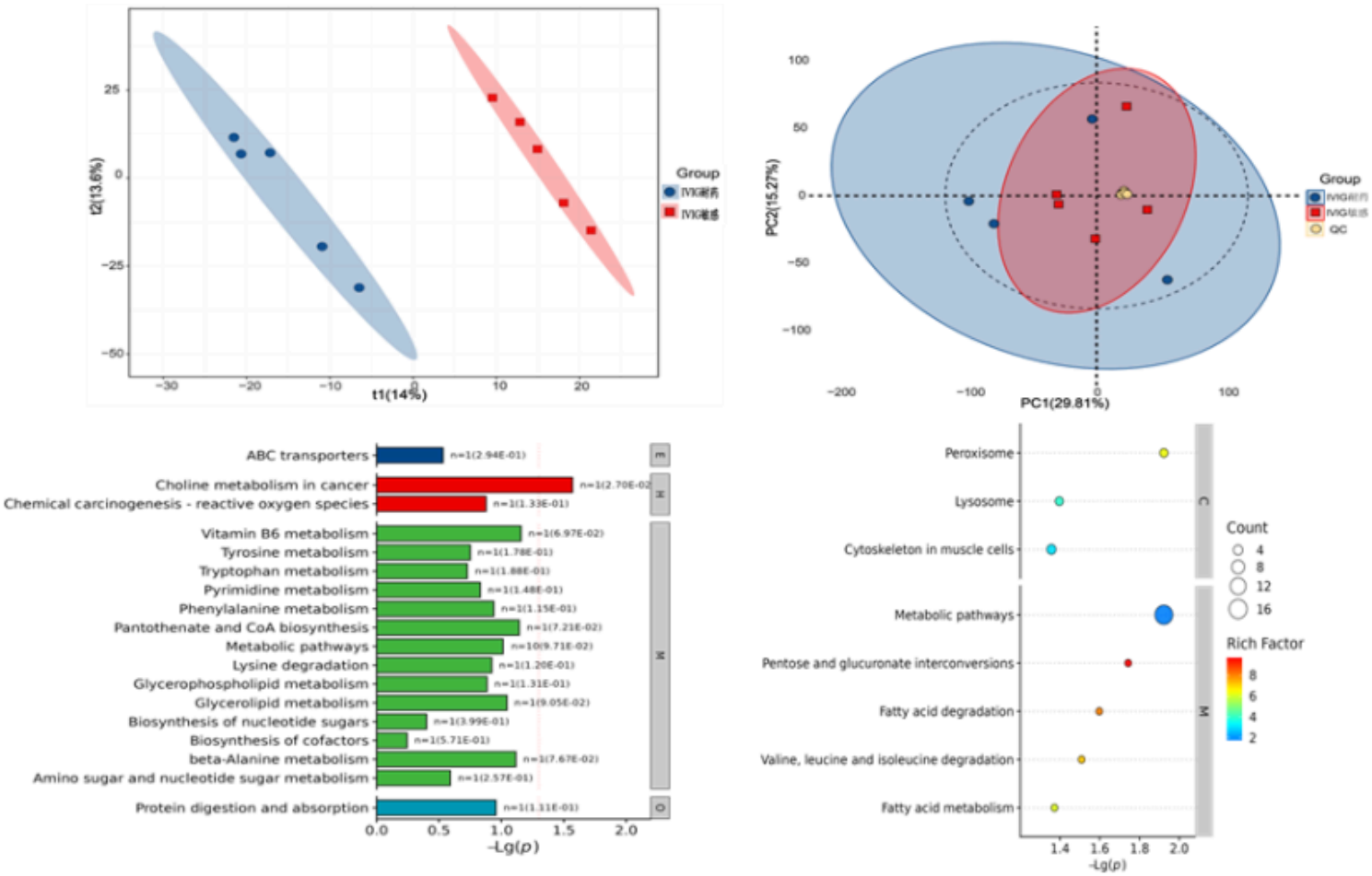


Figure 5

(A) (B): t1 represents principal component 1, t2 represents principal component 2, points of the same color represent various biological replicates within the group, and the distribution of points reflects the degree of difference between and within groups. (C) (D): KEGG pathways enriched with differentially expressed metabolites and proteins, respectively.

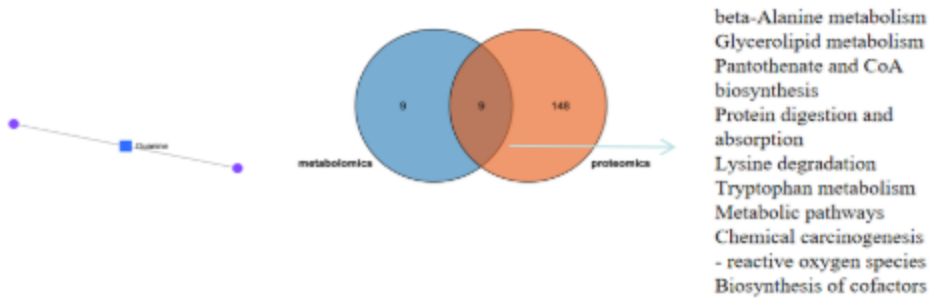


Figure 6

A illustrates the DEMs and DEPs correlation interactions network map in the IVIG-resistant-IVIG-sensitive group, and B illustrates the KEGG pathway that DEMs and DEPs are co-enriched to in the IVIG-resistant-IVIG-sensitive group.

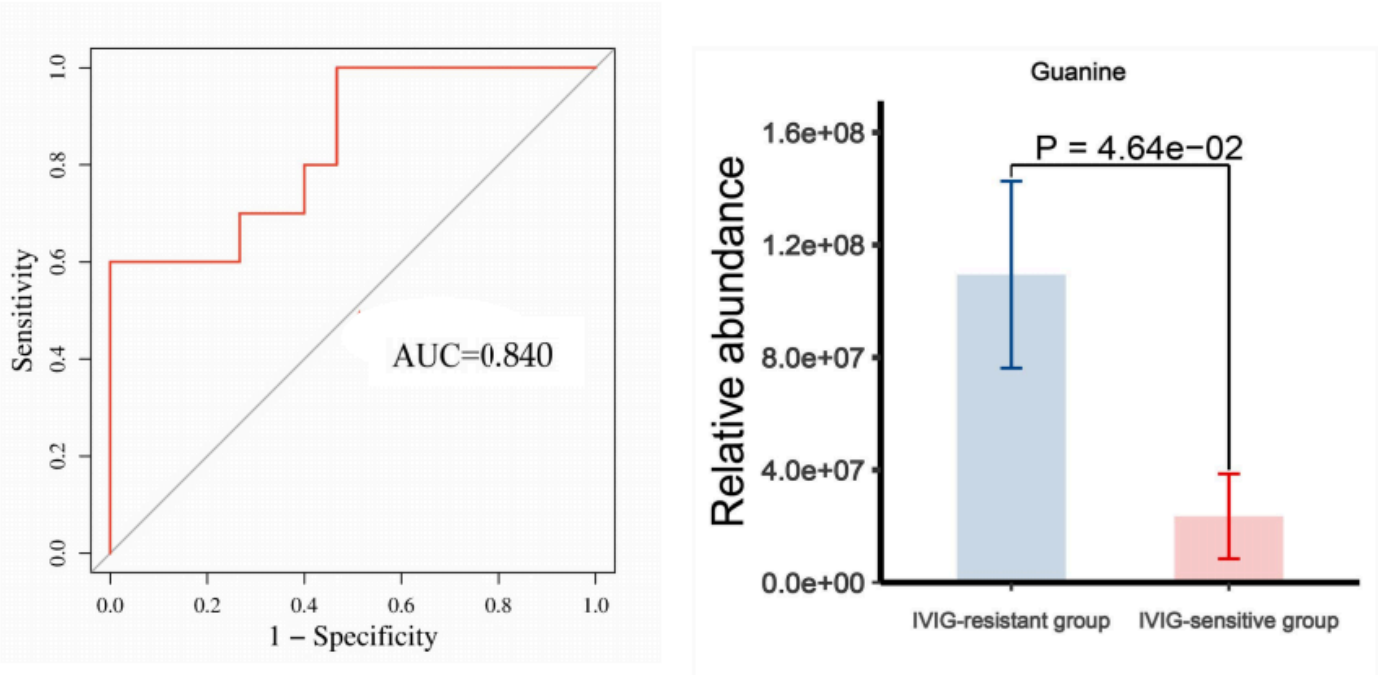


Figure 7

Guanylate roc curves and expression between groups, where group III represents the IVIG-resistant group and group IV represents the IVIG-sensitive group.